nature medicine

Bat3 promotes T cell responses and autoimmunity by repressing Tim-3–mediated cell death and exhaustion

Manu Rangachari[1,10], Chen Zhu[1,10], Kaori Sakuishi[1], Sheng Xiao[1], Jozsef Karman[1,9], Andrew Chen[1], Mathieu Angin[2], Andrew Wakeham[3], Edward A Greenfield[4], Raymond A Sobel[5], Hitoshi Okada[3,6,7], Peter J McKinnon[8], Tak W Mak[3], Marylyn M Addo[2], Ana C Anderson[1] & Vijay K Kuchroo[1]

T cell immunoglobulin and mucin domain–containing 3 (Tim-3) is an inhibitory receptor that is expressed on exhausted T cells during infection with HIV-1 and hepatitis C virus. By contrast, Tim-3 expression and function are defective in multiple human autoimmune diseases. However, the molecular mechanisms modulating Tim-3 function are not well understood. Here we show that human leukocyte antigen B (HLA-B)-associated transcript 3 (Bat3) binds to, and represses the function of, Tim-3. Bat3 protects T helper type 1 (T_H1) cells from galectin-9–mediated cell death and promotes both proliferation and proinflammatory cytokine production. Bat3-deficient T cells have elevated expression of exhaustion-associated molecules such as Tim-3, Lag3, Prdm1 and Pbx3, and Bat3 knockdown in myelin-antigen–specific $CD4^+$ T cells markedly inhibits the development of experimental autoimmune encephalomyelitis while promoting the expansion of a dysfunctional Tim-3^{hi}, interferon-γ (IFN-γ)$^{lo}CD4^+$ cell population. Furthermore, expression of Bat3 is reduced in exhausted Tim-3^+ T cells from mouse tumors and HIV-1–infected individuals. These data indicate that Bat3 acts as an inhibitor of Tim-3–dependent exhaustion and cell death. Bat3 may thus represent a viable therapeutic target in autoimmune disorders, chronic infections and cancers.

IFN-γ–secreting T_H1 $CD4^+$ cells and cytotoxic T type 1 (T_C1) $CD8^+$ cells have an essential role in protection against intracellular pathogens and viruses, and IFN-γ production from lymphocytes is a crucial component of tumor immunosurveillance[1] and resistance to chronic viral infections[2,3]. T_H1 responses to self antigens are, however, thought to promote autoimmune disease in rodents and humans[3,4]. Thus, IFN-γ–producing T cells induce human autoimmune diseases and protect against chronic viral infections and cancers.

Tim-3 (encoded by *Havcr2*) is an inhibitory receptor that is specifically expressed on terminally differentiated T_H1 and T_C1 cells[5] and can trigger cell death on interaction with its ligand, galectin-9 (ref. 6). Tim-3 is crucial for the induction of T cell tolerance *in vivo*[7,8], and defective Tim-3 expression and signaling have been observed in $CD4^+$ T cells isolated from patients with multiple sclerosis[9,10] and colitis[11]. Furthermore, recent findings showed that Tim-3 has a crucial role in the development of T cell exhaustion in chronic viral infections such as HIV[12], hepatitis C virus (HCV)[13], lymphocytic choriomeningitis virus[14] and Friend virus infections[15], as well as in tumor-bearing individuals[16–18]. Notably, the amount of Tim-3 expression on HIV-1–specific T cells correlates with their sensitivity to regulatory T cell–mediated suppression[19].

The galectin-9–Tim-3 axis is thus an important negative regulator of T_H1 and T_C1 cell function that could be exploited therapeutically. Whereas boosting Tim-3 signals could dampen autoimmunity, repressing Tim-3 function could augment immune responses to viral infections and cancers. Developing such strategies requires greater insight into the molecular mechanisms of Tim-3–mediated T cell regulation. Here we identify Bat3 (encoded by *Bag6*) as a binding partner to the Tim-3 intracellular tail. Bat3 protects T_H1 cells from galectin-9–mediated cell death and promotes both proliferation and proinflammatory cytokine production. In contrast, knockdown of Bat3 in myelin-antigen–specific T_H1 cells ablates their function and pathogenicity and promotes T cell exhaustion *in vivo*. Further, Bat3 expression is specifically reduced in exhausted Tim-3^+CD4^+ T cells isolated from mouse tumors and HIV-1–infected individuals. Bat3 thus represents a newly identified repressor of Tim-3 signaling that protects T_H1 responses from Tim-3–mediated inhibition.

RESULTS

Tim-3 binds to Bat3

To identify putative intracellular binding partners for Tim-3, we used a yeast two-hybrid approach to screen a mouse spleen complementary DNA library using the intracellular portion of Tim-3 as bait (**Fig. 1a**). Eleven clones corresponded to Bat3, a proline-rich cytoplasmic protein that regulates mammalian cell proliferation and death[20,21].

[1]Center for Neurologic Diseases, Brigham and Women's Hospital, Harvard Medical School, Boston, Massachusetts, USA. [2]Ragon Institute of MGH, MIT and Harvard, Charlestown, Massachusetts, USA. [3]Campbell Family Breast Cancer Research Institute, Princess Margaret Hospital, Toronto, Ontario, Canada. [4]Dana Farber Cancer Institute, Boston, Massachusetts, USA. [5]Department of Pathology, Stanford University School of Medicine, Stanford, California, USA. [6]Division of Signaling Biology, Ontario Cancer Institute, Toronto, Ontario, Canada. [7]Department of Medical Biophysics, University of Toronto, Toronto, Ontario, Canada. [8]St. Jude Children's Research Hospital, Memphis, Tennessee, USA. [9]Present address: Genzyme Corp., Framingham, Massachusetts, USA. [10]These authors contributed equally to this work. Correspondence should be addressed to V.K.K. (vkuchroo@rics.bwh.harvard.edu).

Received 5 December 2011; accepted 14 June 2012; published online 5 August 2012; corrected online 21 August 2012 (details online); doi:10.1038/nm.2871

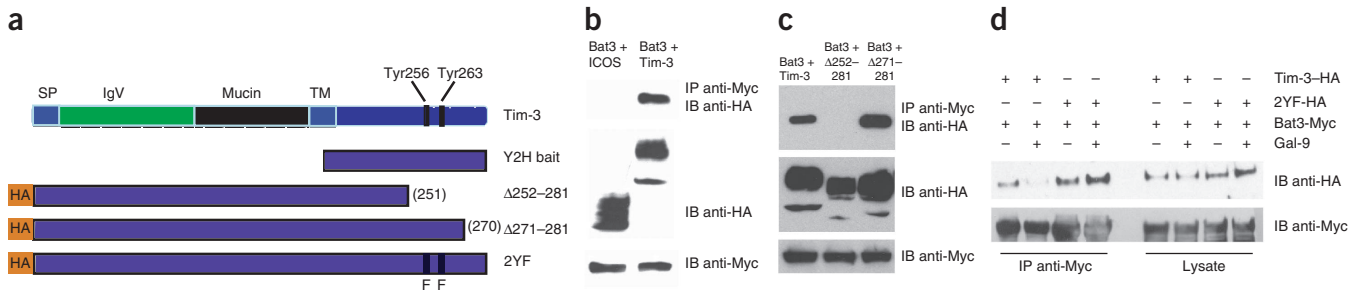

Figure 1 Bat3 binds to the Tim-3 tail in a galectin-9–dependent manner. (**a**) The domain structure and location of the tyrosine residues in the Tim-3 tail and a depiction of the Tim-3 deletion (Tim-$3_{\Delta 252-281}$ and Tim-$3_{\Delta 271-281}$) and substitution constructs (Tim-3_{2YF}) used for yeast two-hybrid (Y2H) screening and coimmunoprecipitation studies. HA, hemagglutinin; SP, signal peptide; TM, transmembrane; F, phenylalanine. (**b**) A western blot of Bat3-Myc and Tim-3–HA (Bat3 + Tim-3) or Bat3-Myc and inducible T cell co-stimulator (ICOS)-HA (Bat3 + ICOS) overexpressed in HEK 293T cells and coimmunoprecipitated to confirm the specificity of the Bat3–Tim-3 interaction in mammalian cells. IP, immunoprecipitation; IB, immunoblot. The anti-prefix indicates antibodies to the indicated factors. The data in **b** are representative of one experiment from eight total. (**c**) A western blot of Bat3-Myc and the HA-tagged Tim-3 deletion mutants HA–Tim-$3_{\Delta 252-281}$ and HA–Tim-$3_{\Delta 271-281}$ expressed in HEK 293T cells and coimmunoprecipitated to elucidate the Bat3-binding domain of Tim-3. Representative of three experiments. (**d**) Cotransfection and coimmunoprecipitation of Bat3, Tim-3 or Tim-3_{2YF} and galectin-9 (Gal-9) constructs in HEK 293T cells. Representative of three experiments.

To confirm the Bat3–Tim-3 interaction, we overexpressed tagged mouse Bat3 and Tim-3 constructs in HEK 293T cells (**Fig. 1a**) and found that Tim-3 coimmunoprecipitated with Bat3 (**Fig. 1b**). Endogenous Tim-3 and Bat3 also coimmunoprecipitated in lymphocytes[22] (**Supplementary Fig. 1**). Using the Tim-3 deletion constructs Tim-$3_{\Delta 252-281}$ and Tim-$3_{\Delta 271-281}$ (**Fig. 1a**), we identified residues 252–270 of Tim-3 as being crucial for mediating binding to Bat3 (**Fig. 1c**). To study a potential role for the Tim-3 ligand galectin-9 in regulating the binding of Bat3 to the Tim-3 tail, we expressed galectin-9 with Bat3 and Tim-3 in HEK 293T cells. Notably, expression of galectin-9 together with Bat3 and Tim-3 abolished the binding of Bat3 to Tim-3 (**Fig. 1d**). As galectin-9 can induce phosphorylation of the Tim-3 tail[23], we tested whether the phosphorylation of residues Tyr256 and Tyr263 is required for the galectin-9–mediated release of Bat3 from Tim-3. A Tim3 complementary DNA in which we replaced these two crucial tyrosines with phenylalanine residues (Tim-3_{2YF}; **Fig. 1a**) could still bind Bat3. However, in contrast to wild-type Tim-3, galectin-9 could not disrupt the binding of Tim-3_{2YF} to Bat3 (**Fig. 1d**). Taken together, our data show that Bat3 binds to residues 252–270 of Tim-3 and that galectin-9 disrupts this interaction by inducing the phosphorylation of two tyrosine residues (Tyr256 and Tyr263) in the Tim-3 tail.

Bat3 protects T_H1 cell responses from inhibition by Tim-3

Using an antisera generated against the N terminus of Bat3 (**Supplementary Fig. 2**), we found that Bat3 is primarily expressed in T_H1 cells (**Fig. 2a**). We observed markedly lower expression of Bat3 in nonpolarized T_H0 cells as well as in polarized T_H17 (**Fig. 2a**) and T_H2 (**Supplementary Fig. 3**) cells. These data, taken together with our finding that galectin-9 abrogates the interaction of Tim-3 with Bat3 (**Fig. 1d**), suggest that Bat3 can regulate the Tim-3 signaling pathway. Notably, we found that Bat3 expression in T_H1 cells is lower in cells that do not express Tim-3 than in those that do (**Supplementary Fig. 4**), suggesting that Tim-3 expression may be required for optimal Bat3 expression in activated T_H1 cells.

In mouse models, Bat3 can have contrasting, context-dependent effects on cell proliferation and survival[20,21]. To determine whether Bat3 repressed or promoted Tim-3–mediated inhibition, we retrovirally overexpressed Bat3 (**Supplementary Fig. 5**) in transgenic 2D2 T_H1

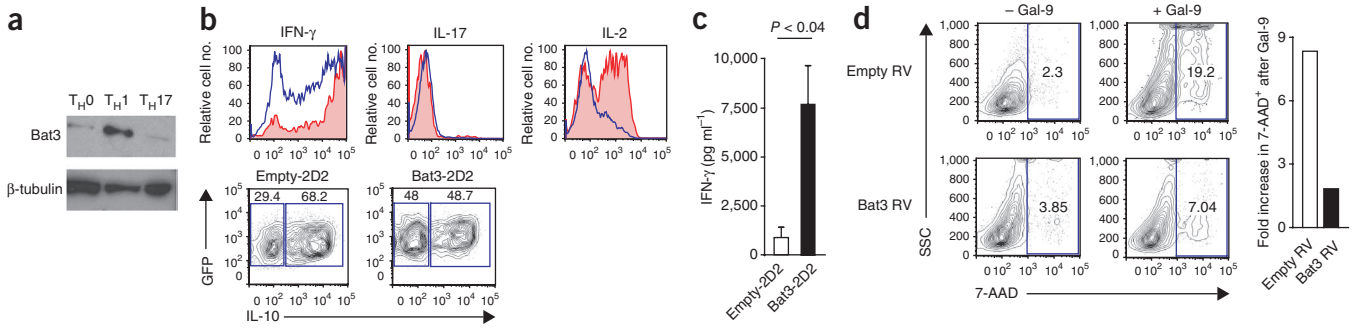

Figure 2 Bat3 promotes T_H1 cell function and protects from galectin-9–mediated cell death. (**a**) Protein expression of Bat3 in C57BL/6 T_H0, T_H1 and T_H17 subsets after 4 d of stimulation, as assessed by reactivity to Bat3 antisera. β-tubulin served as a loading control. Representative of three independent experiments. (**b**) 2D2 $CD4^+$ T cells specific for MOG_{35-55} were polarized under T_H1 conditions, transduced with either empty retrovirus (empty-2D2) or Bat3-expressing retrovirus (Bat3-2D2) and transferred to *Rag1*$^{-/-}$ female recipients. Intracellular expression of IFN-γ, IL-17, IL-2 and IL-10 in GFP^+ cells in splenocytes from these mice 28 d after transfer, as assessed by flow cytometry. The numbers in the IL-10 plots refer to the frequency of $IL\text{-}10^-$ and $IL\text{-}10^+$ cells. In IFN-γ, IL-17 and IL-2 histograms, the blue open areas represent empty-2D2, and the red shaded areas represent Bat3-2D2. (**c**) Concentration of IFN-γ in culture supernatant 48 h after re-stimulation of the splenocytes with MOG_{35-55} peptide. No., number. Data are means ± s.e.m. The *P* value shown was calculated by two-tailed Student's *t* test. (**d**) Frequency of apoptosis (as assessed by 7-aminoactinomycin D (7-AAD)) observed among C57BL/6 T_H1 cells infected with Bat3 or empty retrovirus, successively polarized three times under T_H1 conditions and treated with galectin-9 for 3 h. Numbers contained in the fluorescence-activated cell sorting (FACS) plots represent the frequency of $7\text{-}AAD^+$ cells. SSC, side scatter. Data in the bar graph (right) represent the percentage of $7\text{-}AAD^+$ cells after galectin-9 treatment divided by the percentage of $7\text{-}AAD^+$ cells before treatment. Representative of three experiments.

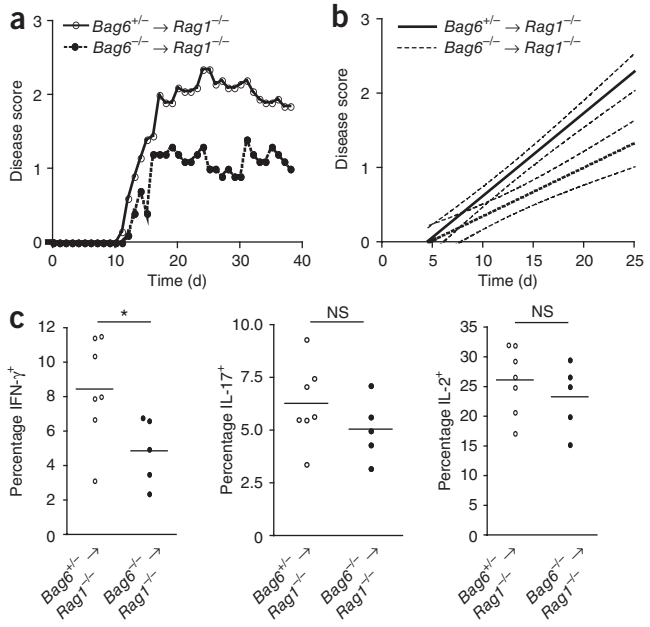

Figure 3 Bat3 expression in the hematopoietic compartment promotes CNS autoimmunity. (**a**) Onset and severity of EAE in *Bag6*$^{+/-}$→*Rag1*$^{-/-}$ and *Bag6*$^{-/-}$→*Rag1*$^{-/-}$ female fetal liver chimeras immunized with MOG_{35-55}. The mean disease score of each group is shown. Results are representative of one of two experiments. *Bag6*$^{+/-}$→*Rag1*$^{-/-}$ mice ($n = 11$), *Bag6*$^{-/-}$→*Rag1*$^{-/-}$ mice ($n = 8$). (**b**) Linear regression curves of the acute phase of the disease are shown for the experiment described in **a**. The slopes are significantly different between the two groups ($P < 0.0001$ by linear regression analysis). The dashed lines indicate the 95% confidence intervals for each curve. (**c**) Frequency of CD4$^+$ T cells expressing either IFN-γ, IL-17 or IL-2 isolated from *Bag6*$^{+/-}$→*Rag1*$^{-/-}$ ($n = 7$) and *Bag6*$^{-/-}$→*Rag1*$^{-/-}$ ($n = 5$) female mice 38 d after MOG_{35-55} immunization. *$P < 0.041$; NS, not significant as measured by two-tailed Student's *t* test. Each data point represents an individual mouse. The horizontal bars contained within the graph represent the mean value for each group.

cells bearing a T cell receptor (TCR) specific for the encephalitogenic myelin oligodendrocyte glycoprotein $(MOG)_{35-55}$ peptide[24]. Using a bicistronic GFP reporter that allowed us to track and purify transduced cells, we sorted and transferred GFP$^+$ retrovirally infected 2D2 T_H1 cells into mice deficient in recombination activating gene 1 (*Rag1*$^{-/-}$ mice), allowed the transferred cells to reconstitute the immune compartment and assessed the function of these cells *ex vivo* 28 d after transfer (**Supplementary Fig. 6**). Bat3-overexpressing 2D2 T_H1 cells produced greater amounts of IFN-γ and interleukin-2 (IL-2) than control cells after *in vivo* expansion (**Fig. 2b**) and significantly more IFN-γ when re-stimulated with MOG_{35-55} ($P < 0.04$; **Fig. 2c**). Neither control cells nor Bat3-overexpressing T_H1 cells produced substantial amounts of IL-17; however, Bat3 overexpression reduced the percentage of T_H1 cells that produced the immunosuppressive cytokine IL-10 (**Fig. 2b**). Notably, mice that received Bat3-overexpressing 2D2 T_H1 cells developed earlier onset experimental autoimmune encephalomyelitis (EAE) that was of greater clinical severity compared to mice that received control 2D2 T_H1 cells (**Supplementary Fig. 7**). Thus, Bat3 overexpression promotes T_H1 cell responses.

To directly assess the effect of Bat3 on signaling through the galectin-9–Tim-3 axis, we assessed the ability of galectin-9 to induce the death of Bat3-overexpressing T_H1 cells. A lower percentage of Bat3-transduced T_H1 cells underwent cell death than did control vector-transduced T_H1 cells after galectin-9 treatment (**Fig. 2d**), suggesting that Bat3 protects T_H1 cells from Tim-3–dependent inhibitory signals both *in vitro* and *in vivo*.

Loss of Bat3 reduces EAE severity

As Bat3 seemed to protect T_H1 cells from the inhibitory functions of Tim-3, loss of Bat3 *in vivo* could dampen autoimmunity by leaving the inhibitory functions of Tim-3 unopposed. We therefore tested the consequences of Bat3 ablation in mouse EAE, an autoimmune disease driven primarily by inflammatory CD4$^+$ cells reactive against myelin antigens[25] that can be induced by T_H1 cells independently of T_H17 cells[26].

Bat3 deficiency results in embryonic lethality in the C57BL/6J mouse strain[20,21]. We therefore generated chimeric mice by transferring *Bag6*$^{+/-}$ or *Bag6*$^{-/-}$ fetal liver cells into *Rag1*$^{-/-}$ mice. We immunized these chimeras with MOG_{35-55} and monitored them for the development of EAE. *Bag6*$^{-/-}$→*Rag1*$^{-/-}$ mice developed disease of significantly lower severity compared to their *Bag6*$^{+/-}$→*Rag1*$^{-/-}$ counterparts ($P < 0.0001$; **Fig. 3a**,**b**), suggesting that Bat3 has an important role in promoting T cell–driven autoimmunity. Further, we observed a significantly lower frequency of IFN-γ–producing ($P < 0.041$), but not IL-17– or IL-2–producing, CD4$^+$ T cells in the peripheral lymphoid tissues of *Bag6*$^{-/-}$→*Rag1*$^{-/-}$ than of *Bag6*$^{+/-}$→*Rag1*$^{-/-}$ MOG-immunized mice (**Fig. 3c**).

Bat3-deficient T cells have an exhausted-like phenotype

To gain a better understanding of the consequences of the loss of function of Bat3 on the generation of effector T cell responses, we isolated CD4$^+$ T cells from *Bag6*$^{+/-}$→*Rag1*$^{-/-}$ and *Bag6*$^{-/-}$→*Rag1*$^{-/-}$ mice in which lymphocytes had expanded homeostatically in a lymphopenic environment. We noted a markedly lower frequency of IFN-γ– and IL-2–producing T cells in the absence of Bat3 expression (**Fig. 4a**). These Bat3-deficient CD4$^+$ T cells also expressed higher amounts of intracellular IL-10 and surface Tim-3 (**Fig. 4a**). This IFN-γ^{lo}IL-2^{lo}IL-10^{hi}Tim-3^{hi} phenotype shares many of the characteristics of exhausted T cells[12–14,16,18,27,28].

A number of groups, including ours, have identified Tim-3 as a functional marker of exhausted T cells[11–18]. Further, T cells with an exhausted-like phenotype have been observed in *Rasgrp1*$^{-/-}$ mice, which are T cell lymphopenic[29]. This raised the possibility that homeostatic expansion of *Bag6*$^{-/-}$ T cells in *Rag1*$^{-/-}$ mice might favor the generation of an exhaustion-like phenotype in these cells. In addition to their high Tim-3 expression, we found that Bat-3–deficient CD4$^+$ T cells upregulated a number of exhaustion-associated markers, such as the transcription factors Prdm1 (ref. 30) and Pbx3 (ref. 31), as well as the T cell exhaustion surface receptor Lag3 (ref. 32) (**Fig. 4b**). These data suggest that in the absence of Bat3, homeostatic expansion of CD4$^+$ T cells in a lymphocyte-deficient environment can result in the development of an exhaustion-like T cell phenotype.

We next explored the potential mechanism(s) of Bat3 function in promoting T_H1 cell responses and in suppressing the generation of T cell exhaustion. We found that Tim-3 is incorporated into supramolecular activation clusters upon T cell activation (data not shown) and that Tim-3 signaling reduces T_H1 cell proliferation (**Supplementary Fig. 8**) and IFN-γ production[33]. We then found that there was higher expression of Tim-3 on Bat3-deficient CD3-ε^{lo}CD4$^+$ T cells as compared to Bat3-sufficient CD3-ε^{lo}CD4$^+$ cells. By contrast, we found no differences in Tim-3 expression between Bat3-deficient and Bat3-sufficient cells in the CD3-ε^{hi} pool of CD4$^+$ T cells (**Fig. 4c**). These data suggest that loss of Bat3 function may favor the generation of a Tim-3$^+$CD3-ε^{lo}CD4$^+$ T cell population.

Tim-3 has recently been described as binding to TCR-associated Src-family kinases that are required for the transduction of TCR-dependent

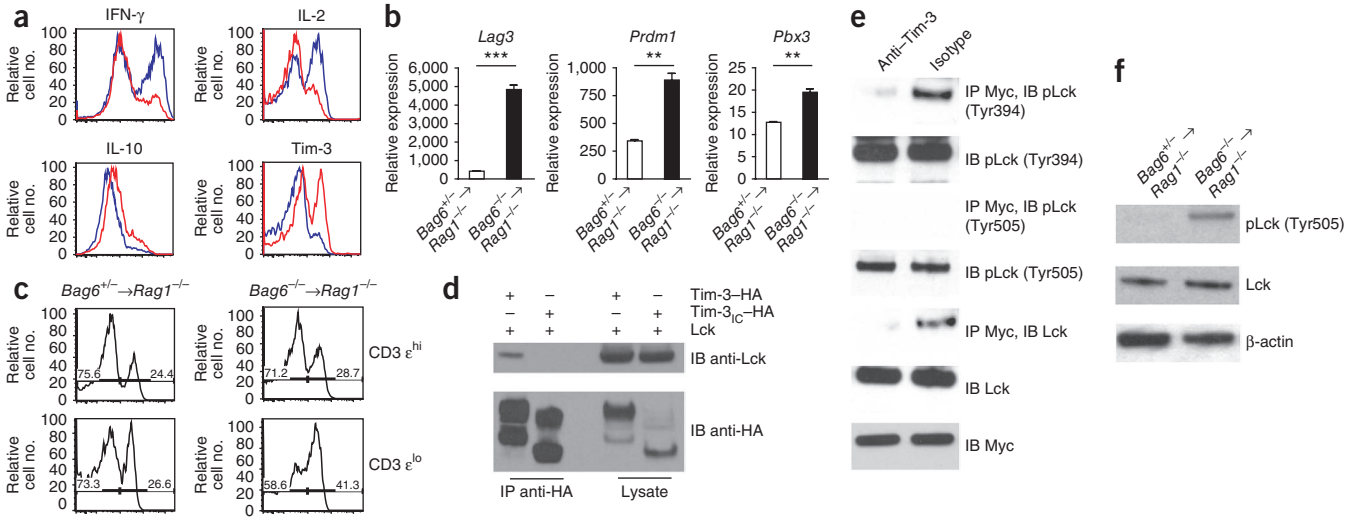

Figure 4 Loss of Bat3 function in T cells induces an exhausted-like phenotype. (**a**,**b**) Analysis of intracellular IFN-γ, IL-2 and IL-10 and surface Tim-3 expression (**a**) and mRNA expression of *Lag3*, *Prdm1* and *Pbx3* (**b**) from *Bag6*$^{+/-}$ and *Bag6*$^{-/-}$ CD4$^+$ T cells that had undergone homeostatic expansion in female *Rag1*$^{-/-}$ host mice for >10 months and were then isolated and re-stimulated *ex vivo* with antibodies to CD3 and CD28. Blue, *Bag6*$^{+/-}$→*Rag1*$^{-/-}$; red, *Bag6*$^{-/-}$→*Rag1*$^{-/-}$ (**a**). *Lag3*, ***$P < 0.0001$; *Prdm1*, **$P < 0.0012$; *Pbx3*, **$P < 0.0088$ by Student's *t* test. Data are means ± s.e.m. (**c**) Cells from **a** gated on CD3-ε expression and analyzed for Tim-3 surface expression. Numbers adjacent to the curves represent the frequency of Tim-3$^-$ and Tim-3$^+$ cells. (**d**) Lck can coimmunoprecipitate wild-type Tim-3, but not Tim-3 lacking its intracellular domain (Tim-3$_{IC}$), when expressed in HEK 293T cells. Data are representative of one experiment among three total. (**e**) Coimmunoprecipitation of Bat3-Myc with pLck (Tyr394) and total Lck, but not with pLck (Tyr505), in T cells after incubation with a Tim-3–specific antibody. Representative of one experiment among three total. (**f**) Expression of pLck (Tyr505) from *Bag6*$^{+/-}$ and *Bag6*$^{-/-}$ CD4$^+$ T cells that were expanded in *Rag1*$^{-/-}$ host mice for >10 months and re-stimulated for 5 d *in vitro* with antibodies to CD3 and CD28. Representative of three experiments.

signals[33]. We found that Tim-3 could bind to the Src homology 3 (SH3)-domain–containing TCR-associated intracellular kinase Lck in a manner that was dependent on the presence of the Tim-3 intracellular tail (**Fig. 4d**). We therefore asked whether Bat3, a proline-rich molecule, could interact with the SH3-domain–containing Lck in a Tim-3–dependent manner and thereby modulate the downstream effects of Tim-3. Bat3 and Lck physically interact when both molecules were expressed in HEK 293 cells (**Supplementary Fig. 9**). When Bat3 is retrovirally overexpressed in activated primary T_H1 cells, it could immunoprecipitate Lck. Notably, this interaction was abrogated when we treated the cells with an antibody to Tim-3 (**Fig. 4e**). When phosphorylated at Tyr394, Lck becomes catalytically active and is able to phosphorylate downstream substrates that promote optimal T cell activation[34]. By contrast, phosphorylation of Lck at Tyr505 renders it catalytically inactive, and it has been proposed that T cell activation is at least partially regulated by the balance of active and inactive Lck within a cell[35]. Notably, Bat3 could pull down the catalytically active form of Lck (phosphorylated at Tyr394 (pTyr394)) in T_H1 cells (**Fig. 4e**). Ligation of the Tim-3 receptor by a Tim-3–specific antibody inhibited this interaction. By contrast, Bat3 could not pull down catalytically inactive Lck in cells treated with the Tim-3–specific antibody or an isotype control. Notably, neither the total amounts of Lck nor the total amounts of phosphorylated Lck were perturbed by treatment with antibody to Tim-3 (**Fig. 4e**). These data indicate that Bat3 can bind and recruit catalytically active Lck to the Tim-3 tail and that receptor ligation of Tim-3 triggers the release of the catalytically active form of Lck from Bat3.

We next asked whether loss of Bat3 could negatively regulate TCR-mediated signaling by increasing the proportion of catalytically inactive Lck in T cells. Although there were low amounts of catalytically inactive Lck (pTyr505) in Bat3-sufficient T cells re-stimulated with antibodies to CD3 and CD28, a substantial amount of catalytically inactive Lck accumulated in Bat3-deficient T cells stimulated with the same antibodies (**Fig. 4f**). Thus, Tim-3, which is recruited to the supramolecular activation cluster during T cell activation, forms an intracellular molecular complex with Bat3 and the catalytically active form of Lck to promote T cell signaling, activation and expansion. However, loss of Bat3 results in the accumulation of the catalytically inactive form of Lck, which parallels the defective IL-2 production found in Bat3-deficient T cells.

Bat3 is crucial to induce T_H1 cell–driven autoimmunity

To study the consequences of loss of Bat3 function exclusively in T_H1 cell–driven autoimmunity, we devised a system for ablating Bat3 expression specifically in myelin-antigen–specific T cells. We generated an shRNA (Bat3KD1) that efficiently knocked down the expression of Bat3 in T cells (**Supplementary Fig. 10**). We then cultured CD4$^+$ T cells under T_H1 polarizing conditions and retrovirally transduced them with either Bat3KD1 (Bat3KD1 2D2 T_H1 cells) or control retrovirus (control 2D2 T_H1 cells). Knockdown of Bat3 had no apparent affect on T cell viability (**Supplementary Fig. 11**). As the retrovirus constructs contained a bicistronic GFP reporter, we sorted GFP$^+$ cells and transferred them into *Rag1*$^{-/-}$ recipient mice. All mice adoptively transferred with control 2D2 T_H1 cells developed EAE, whereas the severity and incidence of EAE was lower in mice adoptively transferred with Bat3KD1 2D2 T_H1 cells (**Fig. 5a** and **Supplementary Table 1**). Furthermore, the number of GFP$^+$CD4$^+$ cells infiltrating the central nervous system (CNS) of mice receiving Bat3KD1 2D2 T_H1 cells was fivefold lower as compared to mice receiving control 2D2 cells (**Fig. 5b**). In addition, we observed significantly fewer inflammatory foci in the meninges ($P < 0.0001$) and CNS ($P < 0.0011$) of mice receiving Bat3KD1 2D2 T_H1 cells than those receiving control 2D2 T_H1 cells (**Supplementary Table 1**). These findings show that Bat3 is crucial for the pathogenicity, survival or both of T_H1 cells and support a role for Bat3 in preserving T_H1 cell function *in vivo*.

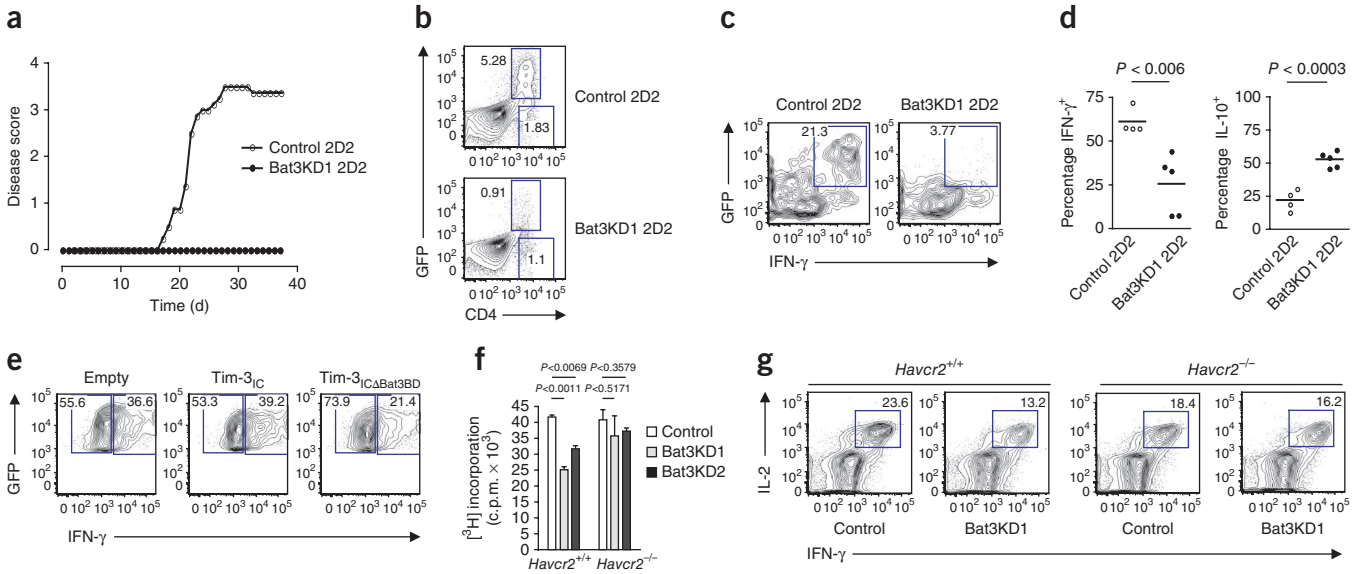

Figure 5 Bat3 expression in CD4$^+$ T cells is required for T_H1 cell–driven EAE. (**a**) EAE onset and severity in female *Rag1*$^{-/-}$ mice that received 2D2 T_H1 cells infected either with control retrovirus or with Bat3KD1 shRNA-containing retrovirus. The data represent one of a total of three transfers. $n = 4$ mice receiving control 2D2 cells, $n = 6$ mice receiving Bat3KD1 2D2 cells. (**b**) GFP and CD4 positivity of CNS-infiltrating mononuclear cells from *Rag1*$^{-/-}$ female mice that received control 2D2 T_H1 cells or Bat3KD1 2D2 T_H1 cells collected at day 38 after transfer. The data are representative of four mice receiving control 2D2 cells or two mice receiving Bat3KD1 2D2 cells. (**c**,**d**) Frequency of IFN-γ$^+$ (**c**,**d**: left) and IL-10$^+$ (**d**: right) lymph node CD4$^+$ cells collected at day 38 after transfer from *Rag1*$^{-/-}$ mice that had received control or Bat3KD1 2D2 T_H1 cells. The plots were gated on CD4$^+$, and the data are representative of four mice receiving control 2D2 cells or five mice receiving Bat3KD1 2D2 cells (**c**). In **d**, each data point represents an individual mouse, and the horizontal bars within the graphs represent the means of each group. *P* values were determined by two-tailed Student's *t* test. (**e**) Intracellular IFN-γ staining in GFP$^+$ T_H1 cells transduced with empty retrovirus, retrovirus expressing Tim-3_{IC} or retrovirus expressing Tim-$3_{IC\Delta Bat3BD}$ 5 d after a second stimulation. Data are from one of three experiments. (**f**) T cell proliferation (as assessed by [^{3}H]-thymidine incorporation) of control-, Bat3KD1- or Bat3KD2-transduced *Havcr2*$^{+/+}$ and *Havcr2*$^{-/-}$ T_H1 cells cultured for 5 d, sorted for GFP positivity and re-stimulated with 1 μg ml^{-1} antibodies to CD3 and CD28 for 48 h. Representative of three experiments. c.p.m., counts per minute. Data are means ± s.e.m. The *P* values shown were calculated by Student's *t* test. (**g**) Intracellular cytokine staining for IFN-γ and IL-2 of control- or Bat3KD1-transduced *Havcr2*$^{+/+}$ and *Havcr2*$^{-/-}$ T_H1 cells cultured for 5 d (gated on GFP$^+$). Representative of three experiments. The numbers associated with the FACS plot gates refer to the frequency of cells contained within each gate.

To assess the functional consequences of Bat3 knockdown on cytokine expression *in vivo*, we analyzed the surface phenotype and cytokine expression of the transferred 2D2 T_H1 cells in the immune and diseased tissues of *Rag1*$^{-/-}$ recipients. Mice receiving control 2D2 T_H1 cells had large numbers of GFP$^+$IFN-γ^{hi}CD4$^+$ T cells in their lymph nodes. By contrast, mice receiving Bat3KD1 2D2 T_H1 cells had very few GFP$^+$IFN-γ^{hi}CD4$^+$ T cells (**Fig. 5c**). Notably, when we analyzed GFP$^+$ T cells (**Supplementary Fig. 12**) for cytokine production, we found that although Bat3KD1 2D2 T_H1 cells produced less IFN-γ than control 2D2 T_H1 cells, they produced substantially more IL-10 (**Fig. 5d**), a phenomenon that has been observed in exhausted T cells[14].

To more closely link the interaction of Bat3 and Tim-3 to the maintenance of T_H1 cell responses, we transduced primary T_H1 cells with retrovirus gene expression constructs encoding the intracellular region of Tim-3 (Tim-3_{IC}) or the intracellular region of Tim-3 lacking the Bat3-binding domain (Tim-$3_{IC\Delta Bat3BD}$), which is located at amino acids 252–281 (**Fig. 1a**,**c**). Expression of Tim-$3_{IC\Delta Bat3BD}$ impaired IFN-γ production in T_H1 cells relative to control T_H1 cells transduced with empty retrovirus or Tim-3_{IC}–expressing retrovirus (**Fig. 5e**). To formally show that the defects in T cell function observed after Bat3 knockdown were dependent on Tim-3, we knocked down Bat3 expression in both *Havcr2*$^{+/+}$ and *Havcr2*$^{-/-}$ T_H1 cells using two different Bat3-specific shRNAs, Bat3KD1 and Bat3KD2 (**Supplementary Fig. 10**). Bat3 knockdown suppressed the proliferation of *Havcr2*$^{+/+}$ T_H1 cells (**Fig. 5f**) but had little effect on the proliferative capacity of *Havcr2*$^{-/-}$ T_H1 cells (**Fig. 5f**). Knockdown of Bat3 also reduced the frequency of IFN-γ$^+$IL-2$^+$ CD4$^+$ cells among *Havcr2*$^{+/+}$, but not *Havcr2*$^{-/-}$, T_H1 cells (**Fig. 5g**). These data indicate that the loss of T cell function (as assessed by proliferative capacity and the production of IFN-γ and IL-2) that accompanies the reduction of Bat3 expression is dependent on Tim-3.

Bat3 expression is reduced in Tim-3$^+$ exhausted T cells

Given the established role of Tim-3 in inducing and maintaining T cell exhaustion[12–18], we asked whether Bat3 was differentially regulated in exhausted Tim-3$^+$ T cells generated *in vivo*. We recently reported that Tim-3 expression characterizes a subpopulation of programmed cell death 1 (PD-1)$^+$ tumor infiltrating lymphocytes (TILs) that are exhausted and have impaired effector functions[16,18]. Tim-3$^+$PD-1$^+$ TILs isolated from both the 4T1 mammary adenocarcinoma (**Fig. 6a**) and CT26 colorectal carcinoma[16] models produce much lower amounts of IFN-γ and tumor necrosis factor α (TNF-α) than Tim-3$^-$PD-1$^+$ TILs. Combined *in vivo* blockade of PD-1 signaling (using an antibody against programmed cell death ligand 1 (PD-L1)) and Tim-3 signaling increased IFN-γ production from TILs relative to either PD-1 or Tim-3 signal blockade alone (**Fig. 6b**). These Tim-3$^+$PD-1$^+$ TILs expressed 50% lower amounts of *Bat3* mRNA relative to Tim-3$^-$PD-1$^+$ cells (**Fig. 6c**). To extend our findings to both chronic viral infections and human disease, we asked whether Bat3 was differentially expressed in Tim-3$^+$ exhausted T cells isolated from untreated HIV-1–infected individuals[12]. We sorted

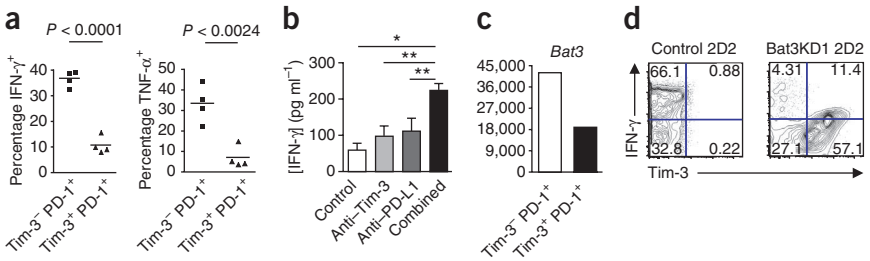

Figure 6 Bat3 expression is reduced in Tim-3$^+$ exhausted T cells. (**a**) Intracellular production of IFN-γ and TNF-α from TILs isolated from female 4T1 mammary adenocarcinoma recipients at 26 d after implantation. Each data point represents an individual mouse. The horizontal bars indicate the mean. *P* values were obtained by two-tailed Student's *t* test. (**b**) IFN-γ concentration in culture supernatants from lymph node T cells isolated from CT26 tumor-bearing female mice treated *in vivo* with the indicated antibodies and stimulated *in vitro* with tumor antigen (AH1) for 48 h. $^*P < 0.05$, $^{**}P < 0.01$. *P* values were calculated by one-way analysis of variance followed by *post hoc* Tukey's multiple comparison test. Data are means ± s.e.m. (**c**) *Bat3* mRNA expression in Tim-3$^+$PD-1$^+$ and Tim-3$^-$PD-1$^+$ TIL subpopulations isolated from ectopic CT26 colorectal carcinomas 21 d after implantation in female mouse recipients. Data were normalized to β-actin. Data represent pooled tumors from ten recipients. (**d**) Tim-3 (surface) and IFN-γ (intracellular) coexpression profiles of lymph node cells isolated 38 d after transfer from *Rag1*$^{-/-}$ female recipient mice receiving either control 2D2 T_H1 cells ($n = 9$) or Bat3KD1 2D2 T_H1 cells ($n = 5$). The plots were gated on CD4 positivity. The numbers contained within the plots refer to the percentage of cells contained within each quadrant.

Tim-3$^-$PD-1$^+$CD4$^+$ and Tim-3$^+$PD-1$^+$CD4$^+$ T cell populations from the blood of three individuals with untreated HIV-1 infection (median HIV-1 viral load of 79,200 RNA copies ml^{-1}, interquartile range 69,630–169,000 copies ml^{-1}). *BAT3* mRNA expression was significantly reduced in Tim-3$^+$PD-1$^+$ exhausted CD4$^+$ cells isolated from all three individuals relative to Tim-3$^-$PD-1$^+$CD4$^+$ T cells (individual 1, $P < 0.024$; individual 2, $P < 0.004$; individual 3, $P < 0.004$; **Supplementary Fig. 13**). An analysis of a larger group of patients is required to ascertain whether there is any correlation between *BAT3* expression in Tim-3$^+$ T cells and viral load. Nevertheless, these data suggest that low *BAT3* expression in T cells correlates with Tim-3 expression *in vivo* and with the development of functional exhaustion in both mouse and man.

Although T cell exhaustion is detrimental in chronic viral infections and cancers, it may have evolved as a mechanism of peripheral tolerance to autoantigens and could thus be highly desirable in the context of autoimmune disorders such as multiple sclerosis. We therefore considered the possibility that downregulation of Bat3 expression could promote an exhaustion-like phenotype in T_H1 cells. We thus tested the effect of Bat3 downregulation on the development of *in vivo* effector T cell responses after adoptive transfer of 2D2 T_H1 cells into *Rag1*$^{-/-}$ mice. The majority of the peripheral CD4$^+$ T cells from mice receiving control 2D2 T_H1 cells were highly IFN-γ positive and did not express Tim-3. In contrast, T cells from 5 of 11 mice receiving Bat3KD1 2D2 T_H1 cells had a higher frequency of Tim-3^{hi}IFN-γ^{lo}CD4$^+$ cells in their peripheral lymphoid compartments (**Fig. 6d**). The small number of IFN-γ^{hi}CD4$^+$ T cells that we isolated from these mice were all Tim-3$^-$(**Fig. 6d**). Notably, the Tim-3$^+$IFN-γ^{lo}CD4$^+$ cells isolated from mice receiving Bat3KD1 2D2 T_H1 cells were also PD-1$^-$ (**Supplementary Fig. 14**). Bat3-deficient T_H1 cells thus resemble the recently described Tim-3$^+$ exhausted T lymphocyte population observed in chronic infections caused by HIV[12] or HCV[13] and in tumors[16,18] in many ways, including low proliferation (**Fig. 5f**), high Tim-3 expression coupled with low IFN-γ production (**Figs. 4a** and **6d**) and high IL-10 production (**Fig. 5d**). Thus, Bat3 may be a regulator of both T cell death and exhaustion in T_H1 cells.

DISCUSSION

Tim-3 is a key negative regulator of T cell function[5,7,8], and dysregulated expression of Tim-3 has been implicated in many pathological conditions, including autoimmune disorders[9–11], chronic viral infections[12–15,19] and malignancies[16–18]. However, in contrast to negative regulatory receptors such as cytotoxic T lymphocyte–associated protein 4 (CTLA-4) (reviewed in ref. 36) and PD-1 (refs. 37–39), little is known about the intracellular molecules that interact with, and modulate the function of, Tim-3. Here we show that the molecular adaptor Bat3 binds to the intracellular tail of Tim-3 and protects T_H1 cells from Tim-3–mediated cell death or exhaustion. Bat3, the mammalian homolog of *Drosophila* Scythe, contains lengthy proline-rich tracts, making it an attractive molecular scaffold that can mediate multiple protein-protein interactions[40–44]. Interestingly, polymorphisms in the Bat3 locus have been linked to increased incidence of type I diabetes[45], suggesting that regulation of Bat3 expression can affect the prevalence of human autoimmune disorders.

Our findings indicate that Bat3 can both promote IFN-γ production *in vivo* and render T_H1 cells resistant to galectin-9–mediated cell death. This suggests that the physical interaction of Bat3 with Tim-3 provides a means by which IFN-γ^{hi} T_H1 cells can be protected from Tim-3–dependent negative regulation. Further, loss or decreased expression of Bat3 in CD4$^+$ T cells reduces their encephalitogenic capacity and leads to the generation of a Tim-3^{hi} exhausted-like T cell population characteristic of that seen in HIV-1 and lymphocytic choriomeningitis virus infection, as well as in the context of mouse and human tumors[12–14,16,18]. Notably, we found low Bat3 expression in both mouse Tim-3$^+$ TILs and in exhausted Tim-3$^+$CD4$^+$ T cells isolated from untreated HIV-1–infected individuals. Promoting the interaction of Bat3 and Tim-3 in exhausted virus- or tumor-specific T cells could reverse their dysfunction. Further, our data point toward a new and possibly promising strategy in autoimmune therapy. By augmenting Tim-3 signaling in autoaggressive T cells, an inflammatory response that is characterized by tissue infiltration could potentially be shifted toward an exhausted response that is characterized by loss of T cell effector functions.

Taken together, our findings suggest that Bat3 promotes T_H1 effector responses by binding to and inhibiting Tim-3. The interaction of Tim-3 with its ligand galectin-9 abrogates the Bat3–Tim-3 binding activity, allowing Tim-3 to transduce inhibitory signals that limit T_H1 effector responses and potentially induce T cell exhaustion. Manipulation of the interaction between Bat3 and Tim-3 could be a promising molecular target for therapeutic intervention in autoimmune disease, cancer and chronic viral infections.

METHODS

Methods and any associated references are available in the online version of the paper.

Note: Supplementary information is available in the online version of the paper.

ACKNOWLEDGMENTS

We thank D. Kozoriz, D. Lee, J. Sullivan and M. King for technical assistance; J. Zhang (Brigham and Women's Hospital, Boston) for reagents; B.H. Waksman for valuable guidance and discussion; and B. Walker for critical reading of the manuscript. M.R. was previously supported by Fellowships from the Multiple Sclerosis Society of Canada (MSSOC) and the Canadian Institutes of Health Research (CIHR) and is currently supported by the EMD Serono, Canada and an MS Research and Training Network Transitional Career Development Award from the MSSOC and the Multiple Sclerosis Scientific Research Foundation. K.S. holds a Fellowship from the Sankyo Foundation of Life Science. These studies were funded by grants from the US National Institutes of Health to V.K.K. (NS045937, AI073748 and NS038037) and S.X. (K01DK090105), the Ragon Institute of MGH, MIT and Harvard (V.K.K., C.Z. and M.M.A.), the American Cancer Society (A.C.A.) and the Harvard University Center for AIDS Research (M.M.A.; P30 AI060354).

AUTHOR CONTRIBUTIONS

M.R. and C.Z. designed and performed experiments, and collected data. M.R. wrote the manuscript. K.S., S.X., J.K., A.C. and M.A. provided help in performing experiments. A.W. helped generate fetal liver chimeric mice. E.A.G. helped generate Bat3 antiserum. R.A.S. analyzed histopathological data. H.O. generated the *Bag6*$^{-/-}$ strain. P.J.M. and T.W.M. provided *Bag6*$^{+/-}$ mice and fetal liver chimeras, respectively. M.M.A. and A.C.A. designed and supervised experiments involving HIV samples and tumor mice, respectively. V.K.K. supervised the project and edited the manuscript.

COMPETING FINANCIAL INTERESTS

The authors declare no competing financial interests.

Published online at http://www.nature.com/doifinder/10.1038/nm.2871.
Reprints and permissions information is available online at http://www.nature.com/reprints/index.html.

1. Dunn, G.P. *et al.* Interferon-γ and cancer immunoediting. *Immunol. Res.* **32**, 231–245 (2005).
2. Myrmel, H., Ulvestad, E. & Asjo, B. The hepatitis C virus enigma. *APMIS* **117**, 427–439 (2009).
3. Romagnani, S. Th1/Th2 cells. *Inflamm. Bowel Dis.* **5**, 285–294 (1999).
4. Moss, R.B. *et al.* Th1/Th2 cells in inflammatory disease states: therapeutic implications. *Expert Opin. Biol. Ther.* **4**, 1887–1896 (2004).
5. Monney, L. *et al.* Th1-specific cell surface protein Tim-3 regulates macrophage activation and severity of an autoimmune disease. *Nature* **415**, 536–541 (2002).
6. Zhu, C. *et al.* The Tim-3 ligand galectin-9 negatively regulates T helper type 1 immunity. *Nat. Immunol.* **6**, 1245–1252 (2005).
7. Sabatos, C.A. *et al.* Interaction of Tim-3 and Tim-3 ligand regulates T helper type 1 responses and induction of peripheral tolerance. *Nat. Immunol.* **4**, 1102–1110 (2003).
8. Sánchez-Fueyo, A. *et al.* Tim-3 inhibits T helper type 1-mediated auto- and alloimmune responses and promotes immunological tolerance. *Nat. Immunol.* **4**, 1093–1101 (2003).
9. Koguchi, K. *et al.* Dysregulated T cell expression of TIM3 in multiple sclerosis. *J. Exp. Med.* **203**, 1413–1418 (2006).
10. Yang, L., Anderson, D.E., Kuchroo, J. & Hafler, D.A. Lack of TIM-3 immunoregulation in multiple sclerosis. *J. Immunol.* **180**, 4409–4414 (2008).
11. Morimoto, K. *et al.* Dysregulated upregulation of T-cell immunoglobulin and mucin domain-3 on mucosal T helper 1 cells in patients with Crohn's disease. *Scand. J. Gastroenterol.* **46**, 701–709 (2011).
12. Jones, R.B. *et al.* Tim-3 expression defines a novel population of dysfunctional T cells with highly elevated frequencies in progressive HIV-1 infection. *J. Exp. Med.* **205**, 2763–2779 (2008).
13. Golden-Mason, L. *et al.* Negative immune regulator Tim-3 is overexpressed on T cells in hepatitis C virus infection and its blockade rescues dysfunctional CD4$^+$ and CD8$^+$ T cells. *J. Virol.* **83**, 9122–9130 (2009).
14. Jin, H.T. *et al.* Cooperation of Tim-3 and PD-1 in CD8 T-cell exhaustion during chronic viral infection. *Proc. Natl. Acad. Sci. USA* **107**, 14733–14738 (2010).
15. Takamura, S. *et al.* Premature terminal exhaustion of Friend virus-specific effector CD8$^+$ T cells by rapid induction of multiple inhibitory receptors. *J. Immunol.* **184**, 4696–4707 (2010).
16. Sakuishi, K. *et al.* Targeting Tim-3 and PD-1 pathways to reverse T cell exhaustion and restore anti-tumor immunity. *J. Exp. Med.* **207**, 2187–2194 (2010).
17. Fourcade, J. *et al.* Upregulation of Tim-3 and PD-1 expression is associated with tumor antigen-specific CD8$^+$ T cell dysfunction in melanoma patients. *J. Exp. Med.* **207**, 2175–2186 (2010).
18. Zhou, Q. *et al.* Co-expression of Tim-3 and PD-1 identifies a CD8$^+$ T-cell exhaustion phenotype in mice with disseminated acute myelogenous leukemia. *Blood* **117**, 4501–4510 (2011).
19. Elahi, S. *et al.* Protective HIV-specific CD8$^+$ T cells evade T_{reg} cell suppression. *Nat. Med.* **17**, 989–995 (2011).
20. Desmots, F., Russell, H.R., Lee, Y., Boyd, K. & McKinnon, P.J. The reaper-binding protein scythe modulates apoptosis and proliferation during mammalian development. *Mol. Cell. Biol.* **25**, 10329–10337 (2005).
21. Sasaki, T. *et al.* HLA-B–associated transcript 3 (Bat3)/Scythe is essential for p300-mediated acetylation of p53. *Genes Dev.* **21**, 848–861 (2007).
22. Kuchroo, V.K. *et al.* Experimental allergic encephalomyelitis mediated by cloned T cells specific for a synthetic peptide of myelin proteolipid protein. Fine specificity and T cell receptor V β usage. *J. Immunol.* **148**, 3776–3782 (1992).
23. van de Weyer, P.S. *et al.* A highly conserved tyrosine of Tim-3 is phosphorylated upon stimulation by its ligand galectin-9. *Biochem. Biophys. Res. Commun.* **351**, 571–576 (2006).
24. Bettelli, E. *et al.* Myelin oligodendrocyte glycoprotein-specific T cell receptor transgenic mice develop spontaneous autoimmune optic neuritis. *J. Exp. Med.* **197**, 1073–1081 (2003).
25. Tsunoda, I. & Fujinami, R.S. Two models for multiple sclerosis: experimental allergic encephalomyelitis and Theiler's murine encephalomyelitis virus. *J. Neuropathol. Exp. Neurol.* **55**, 673–686 (1996).
26. Jäger, A., Dardalhon, V., Sobel, R.A., Bettelli, E. & Kuchroo, V.K. Th1, Th17, and Th9 effector cells induce experimental autoimmune encephalomyelitis with different pathological phenotypes. *J. Immunol.* **183**, 7169–7177 (2009).
27. Wherry, E.J. T cell exhaustion. *Nat. Immunol.* **12**, 492–499 (2011).
28. Blackburn, S.D. & Wherry, E.J. IL-10, T cell exhaustion and viral persistence. *Trends Microbiol.* **15**, 143–146 (2007).
29. Priatel, J.J. *et al.* Chronic immunodeficiency in mice lacking RasGRP1 results in CD4 T cell immune activation and exhaustion. *J. Immunol.* **179**, 2143–2152 (2007).
30. Shin, H. *et al.* A role for the transcriptional repressor Blimp-1 in CD8$^+$ T cell exhaustion during chronic viral infection. *Immunity* **31**, 309–320 (2009).
31. Wherry, E.J. *et al.* Molecular signature of CD8$^+$ T cell exhaustion during chronic viral infection. *Immunity* **27**, 670–684 (2007).
32. Blackburn, S.D. *et al.* Coregulation of CD8$^+$ T cell exhaustion by multiple inhibitory receptors during chronic viral infection. *Nat. Immunol.* **10**, 29–37 (2009).
33. Lee, J. *et al.* Phosphotyrosine-dependent coupling of Tim-3 to T-cell receptor signaling pathways. *Mol. Cell. Biol.* **31**, 3963–3974 (2011).
34. Mustelin, T. & Tasken, K. Positive and negative regulation of T-cell activation through kinases and phosphatases. *Biochem. J.* **371**, 15–27 (2003).
35. Nika, K. *et al.* Constitutively active Lck kinase in T cells drives antigen receptor signal transduction. *Immunity* **32**, 766–777 (2010).
36. Oosterwegel, M.A., Greenwald, R.J., Mandelbrot, D.A., Lorsbach, R.B. & Sharpe, A.H. CTLA-4 and T cell activation. *Curr. Opin. Immunol.* **11**, 294–300 (1999).
37. Okazaki, T., Maeda, A., Nishimura, H., Kurosaki, T. & Honjo, T. PD-1 immunoreceptor inhibits B cell receptor–mediated signaling by recruiting src homology 2-domain-containing tyrosine phosphatase 2 to phosphotyrosine. *Proc. Natl. Acad. Sci. USA* **98**, 13866–13871 (2001).
38. Chemnitz, J.M., Parry, R.V., Nichols, K.E., June, C.H. & Riley, J.L. SHP-1 and SHP-2 associate with immunoreceptor tyrosine-based switch motif of programmed death 1 upon primary human T cell stimulation, but only receptor ligation prevents T cell activation. *J. Immunol.* **173**, 945–954 (2004).
39. Yokosuka, T. *et al.* Programmed cell death 1 forms negative costimulatory microclusters that directly inhibit T cell receptor signaling by recruiting phosphatase SHP2. *J. Exp. Med.* **209**, 1201–1217 (2012).
40. Thress, K., Song, J., Morimoto, R.I. & Kornbluth, S. Reversible inhibition of Hsp70 chaperone function by Scythe and Reaper. *EMBO J.* **20**, 1033–1041 (2001).
41. Winnefeld, M. *et al.* Human SGT interacts with Bag-6/Bat-3/Scythe and cells with reduced levels of either protein display persistence of few misaligned chromosomes and mitotic arrest. *Exp. Cell Res.* **312**, 2500–2514 (2006).
42. Desmots, F., Russell, H.R., Michel, D. & McKinnon, P.J. Scythe regulates apoptosis-inducing factor stability during endoplasmic reticulum stress-induced apoptosis. *J. Biol. Chem.* **283**, 3264–3271 (2008).
43. Tsukahara, T. *et al.* Scythe/BAT3 regulates apoptotic cell death induced by papillomavirus binding factor in human osteosarcoma. *Cancer Sci.* **100**, 47–53 (2009).
44. Kwak, J.H., Kim, S.I., Kim, J.K. & Choi, M.E. BAT3 interacts with transforming growth factor-β (TGF-β) receptors and enhances TGF-β1–induced type I collagen expression in mesangial cells. *J. Biol. Chem.* **283**, 19816–19825 (2008).
45. Degli-Esposti, M.A. *et al.* Ancestral haplotypes reveal the role of the central MHC in the immunogenetics of IDDM. *Immunogenetics* **36**, 345–356 (1992).

ONLINE METHODS

Primary T cell culture, differentiation and functional analysis. $CD4^+$ and $CD8^+$ T cells were enriched from mouse spleen or lymph node single-cell suspensions using MACS magnetic beads (Miltenyi). For some experiments, we labeled cells with fluorescent markers and sorted them using a FACSAria digital cell sorter (Becton Dickinson). Cells were cultured in DMEM (Invitrogen) and supplemented as previously described[7]. For T_H cell differentiation, we stimulated $CD4^+$ T cells with plate-bound antibodies to CD3 and CD28 under T_H0, T_H1 (IL-12 plus blocking antibodies to IL-4) or T_H2 (IL-4 plus blocking antibodies to IFN-γ) conditions. For T_H17 polarization, we purified and stimulated $CD4^+CD62L^{hi}CD25^-$ cells with antibodies to CD3 and CD28, plus transforming growth factor β (TGF-β) and IL-6. After 2 d, cells were transferred to uncoated plates with IL-2 (T_H0, T_H1 and T_H2) or IL-23 (T_H17). For additional rounds of polarization, we re-stimulated cells with plate-bound antibodies and the appropriate cytokines and blocking antibodies 5 d after the initial stimulation. For antigen-specific assays, T cells were stimulated with $MOG_{35–55}$ (1 μg ml^{-1}) or tumor antigen AH1 (20 μg ml^{-1}) and gamma-irradiated splenocytes at a ratio of one T cell to five splenocytes. The supernatant was collected at 48 h for IFN-γ ELISA, and if necessary, cells were then pulsed for 16 h with 1.25 μCi per well $[^3H]$-thymidine (PerkinElmer) for proliferation assays.

Real-time PCR. Total RNA was extracted from target cells and tissues using RNeasy reagents (QIAGEN), and reverse transcription was performed using iScript Reverse Transcriptase (Bio-Rad). Real-time PCR was done using validated primer-probe sets to mouse *Bat3* (*Bag6*), *Lag3*, *Prdm1* or *Pbx3*, human *BAT3*, the appropriate endogenous control *Actb* (mouse) or *GAPDH* (human) primer-probe sets, TaqMan FAST mix and a 7500 real-time PCR cycler (all Applied Biosystems), as previously described[5].

Surface marker and intracellular cytokine staining analysis. We labeled cells with fluorochrome-labeled antibodies against surface markers at 4 °C. For intracellular cytokine staining, cells were re-stimulated for 4 h with 50 ng ml^{-1} phorbol 12-myristate 13-acetate and 1 μM ionomycin (both Sigma) in the presence of GolgiStop (BD; 0.67 μl/ml culture). Cells were then fixed, permeabilized and stained for intracellular markers using the Fixation/Permeabilization Kit (BD). After more than two washes, cells were analyzed using a BD LSRII digital flow cytometer. Negative staining was determined using the appropriate isotype control antibody. Cell death was measured by 7-AAD (BD) positivity. All flow cytometric data were analyzed using FlowJo software (Treestar).

Retroviral transduction. Retroviral expression constructs were transfected into HEK 293T cells along with eco and gag-pol viral envelope constructs. The viral supernatant was collected 48 h after transfection and added to primary T cells that had been activated with plate-bound antibodies to CD3 and CD28 for 24 h. Cells were spun at 2,000 rpm in the presence of polybrene (Sigma; 8 μg ml^{-1}) for 45 min at room temperature and were then returned to 37 °C. GFP^+ cells could be detected 2–3 d after infection.

Mice and induction of EAE. Seven- to 10-week-old C57BL/6, SJL, BALB/cJ and *Rag*$^{-/-}$ mice were purchased from the Jackson Laboratory. $MOG_{35–55}$ antigen–specific 2D2 mice[24], *Havcr2*$^{-/-}$ mice[8] and *Bag6*$^{-/-}$ mice[21] have been described previously. *Rag1*$^{-/-}$ mice were sublethally irradiated and reconstituted with *Bag6*$^{+/-}$ or *Bag6*$^{-/-}$ fetal liver hematopoietic cells, as previously described[46]. All mice used for experiments were female unless otherwise indicated in the figure legends. We induced EAE by subcutaneous injection of the mice with 100 μl of an emulsion containing complete Freund's adjuvant, 250 μg *Mycobacterium tuberculosis* extract H37-Ra (Difco) and 100 μg $MOG_{35–55}$ (MEVGWYRSPFSRVVHLYRNGK; QCB BioSource International). Mice received 200 ng pertussis toxin (List Biological Laboratories) intraperitoneally (i.p.) on days 0 and 2. For cell transfer experiments, 2D2 T_H1 cells were retrovirally transduced and then sorted on GFP^+ 5 d after the initial stimulation. Sorted 2D2 T cells were >98% GFP^+ at the time of transfer. Two million GFP^+ cells were transferred intravenously to each *Rag*$^{-/-}$ recipient. All mice received 200 ng of pertussis toxin (List Biological Laboratories) i.p. at days 0 and 2. The mice were monitored daily for development of EAE and scored using the following criteria: 0, no disease; 1, decreased tail tone; 2, hind limb weakness or partial paralysis; 3, complete hind limb paralysis; 4, front and hind limb paralysis; or 5, moribund state. Mice were killed at the indicated time points. All mice were housed in a specific pathogen–free animal facility. All breeding and experiments were reviewed and approved by the Harvard Medical Area Standing Committee on Animals and were performed in accordance with the US National Institutes of Health guidelines for the use of live animals.

Isolation of TILs. Five-hundred thousand CT26 colorectal carcinoma cells or 1×10^5 4T1 mammary adenocarcinoma cells were implanted subcutaneously into the right flanks of wild-type female BALB/c mice. We isolated TILs by dissociating tumor tissue in the presence of 2.5 mg ml^{-1} collagenase D for 20 min before centrifugation on a discontinuous Percoll gradient (GE Healthcare). For some experiments, mice were injected i.p. with 100 μg Tim-3–specific blocking antibody (days 0, 2 and 4) and/or 200 μg PD-L1–blocking antibody (days 0, 3, 6, 9 and 12) or with the appropriate isotype control antibody.

Statistical evaluation. A two-tailed, unpaired, Student's *t* test was used for statistical evaluations of normally distributed data. Disease incidence data were analyzed using Fisher's exact test. Maximal disease scores were analyzed using the Mann-Whitney *U* test. To assess the differential onset of disease between *Bag6*$^{+/-}$→*Rag1*$^{-/-}$ and *Bag6*$^{-/-}$→*Rag1*$^{-/-}$ mice, a linear regression analysis was performed to determine the slope of the disease onset curve.

Additional methods. Detailed methodology is described in the **Supplementary Methods**.

46. Hara, H. *et al.* The apoptotic protease-activating factor 1–mediated pathway of apoptosis is dispensable for negative selection of thymocytes. *J. Immunol.* **168**, 2288–2295 (2002).